Int. J. Heat Mass Transfer. Vol. 28, No. 7, pp. 1317–1326, 1985
Printed in Great Britain

0017-9310/85 $3.00 + 0.00
Pergamon Press Ltd.

Ductflow heat transfer at a smooth wall which faces a wall covered by protuberances

E. M. SPARROW and D. R. OTIS, Jr.
Department of Mechanical Engineering, University of Minnesota, Minneapolis, MN 55455, U.S.A.

(*Received* 22 *October* 1984 *and in final form* 2 *January* 1985)

Abstract—Measurements were made to determine quasi-local heat transfer coefficients at the smooth principal wall of a flat rectangular duct whose other principal wall is covered by an array of blocklike elements (to be termed modules). The hydraulic-diameter Reynolds number ranged from about 3000 to 18,000. The fully developed Nusselt numbers agreed well with those for smooth-walled ducts when the hydraulic diameter was based on the rectangular cross-section between the tops of the modules and the smooth wall. Heating at both the smooth wall and the modules yielded slightly higher coefficients than did heating at the smooth wall alone. The enhancement of the smooth-wall heat transfer by barriers seated in the space between successive rows of modules was investigated. Substantial enhancement was achieved at the lower Reynolds numbers and for the higher barriers. The major enhancement did not occur immediately after a barrier but, rather, farther downstream, at the point where the barrier-induced separated flow reattached to the smooth wall.

INTRODUCTION

IN CERTAIN cooling applications, notably in the forced convection cooling of electronic equipment, the flow passages are flat rectangular ducts whose two principal walls have distinctly different geometrical characteristics. Such an instance may be encountered when a cooling passage for airflow is formed by two parallel walls, each of which consists of an array of circuitboards placed end-to-end. In practice, it is common to use a number of such passages in parallel to accomplish the required cooling task.

In an important class of circuitboards, blocklike elements (often referred to as modules) are mounted on one surface of the board while the other surface of the board is relatively smooth. When such circuitboards are assembled to form a flow passage, the smooth surface of one board faces the module-covered surface of the opposite board. Therefore, the passage is bounded on one side by a smooth surface and on the other side by a surface having streamwise and spanwise periodic depressions (i.e. the spaces between the modules).

The forced convection heat transfer characteristics of the module-covered surface have been experimentally investigated in the literature (e.g. [1, 2]). The present research is concerned with the heat transfer characteristics of the smooth surface.

To separate the hydrodynamic interactions between the walls from the thermal interactions, heat transfer measurements at the smooth wall have been made both with and without heating at the module-covered wall. For both sets of experiments, the Reynolds number of the airflow was varied by a factor of five. The heat transfer results will be compared with literature information for flat rectangular ducts in which both principal walls are smooth.

In another facet of the research, the response of the heat transfer at the smooth wall to enhancement devices is investigated. The enhancement is promoted by a barrier which is seated in the space between two successive rows of modules and protrudes into the flow passage, directing the airstream toward the smooth wall. Experiments were performed with both a single barrier and a pair of barriers. Two different barrier heights were employed, and for the barrier pairs, the interbarrier separation was varied parametrically. In response to unexpected results related to the presence of the barriers, supplementary experiments were performed in which heat transfer was suppressed upstream of the axial location of the barrier.

THE EXPERIMENTS

Apparatus

A schematic diagram of the experimental apparatus is presented in Fig. 1. The (a) part of the figure is a side view of a representative portion of the flat rectangular duct used in the experiments. Along one of the walls (the lower wall), blocklike modules were deployed in a regular pattern which is streamwise periodic with a period length P. As seen in the top view pictured in the (b) part of the figure, the modules were square blocks (side L) and were also deployed uniformly and periodically in the spanwise direction. The module thickness was t, and the intermodule spacing, identical in the spanwise and streamwise directions, was S.

As noted earlier, barriers were used in certain sets of experiments to investigate the possible enhancement of the heat transfer at the smooth wall. A typical barrier installation is depicted in the side and top views of Fig. 1. As seen there, a barrier is a bar of thickness S seated in the space between two consecutive rows of modules (note that the barrier is continuous in the spanwise direction). The distance to which a barrier protruded into the flow space above the modules is denoted by B. When pairs of barriers were used, they were separated by either one, two, or three modules.

NOMENCLATURE

A	transfer surface area	Sh_{fd}	fully developed value of Sh
B	barrier protrusion into flow, Fig. 1	Sh_D	Sherwood number, $KD/\mathscr{D}$
D	hydraulic diameter, $4HW/2(H+W)$	$Sh_{D,fd}$	fully developed value of Sh_D
$\mathscr{D}$	mass diffusion coefficient	t	module thickness
H	distance between tops of modules and smooth wall, Fig. 1	V^*	superficial velocity, $\dot{w}/\rho(WH)$
		W	duct width
K	mass transfer coefficient	$\dot{w}$	mass flowrate
L	side length of a module	X	streamwise coordinate.
$\dot{M}$	mass transfer rate		
P	streamwise length of a period, Fig. 1	Greek symbols	
$\dot{Q}$	volume flowrate of air	μ	viscosity
Re	Reynolds number, $\dot{w}/\mu W$	ν	kinematic viscosity
Re_D	Reynolds number, V^*D/ν	ρ	density
S	intermodule spacing	ρ_{nb}	bulk density of naphthalene vapor
Sc	Schmidt number	ρ_{nw}	density of naphthalene vapor at wall
Sh	Sherwood number, $KH/\mathscr{D}$	$\Delta\rho_n$	density difference, $(\rho_{nw}-\rho_{nb})$.

The primary focus of the research was the heat transfer at the smooth wall of the duct. As indicated by the tick marks, the smooth wall (i.e. the upper wall) was subdivided into streamwise segments of length P (equal to the period of the module array). Note that each segment spanned the full width W of the duct. Each segment served as an individual measurement zone, such that the average heat transfer coefficient was determined for each segment. The per-segment transfer coefficients will be regarded as quasi-local.

In actuality, the experimental work was carried out using a mass transfer technique—naphthalene sublimation. In view of the well-established analogy between heat and mass transfer, the dimensionless mass transfer coefficients (i.e. the Sherwood numbers) determined in these experiments can be regarded as Nusselt numbers for heat transfer. Note that the boundary condition at the mass transfer surfaces corresponds to uniform wall temperature in the analogous heat transfer problem, so that, strictly speaking, the Nusselt numbers obtained from the analogy correspond to that boundary condition. However, for well-mixed flows (e.g. turbulent flows), the Nusselt numbers are insensitive to the specifics of the thermal boundary conditions.

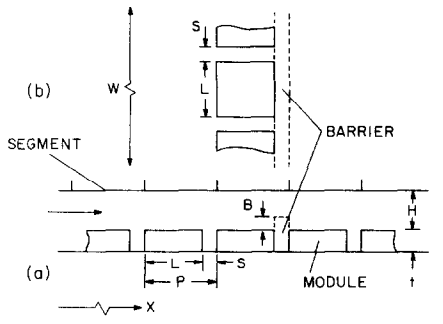

FIG. 1. Schematic diagram of the test section: (a) side view, (b) top view.

Each of the smooth-wall segments was a rectangular slab of naphthalene prepared by a casting process described in detail in [3]. The exposed surface of each slab (i.e. the surface over which the airflow passed) was cast against a highly polished stainless-steel plate, so that the smoothness of the surface was comparable to that of the plate. A fine-gage thermocouple was cast into two of the segments to measure the temperature of the exposed surface.

The ensemble of naphthalene slabs which made up the smooth wall was backed by a precisely machined, thick-walled aluminum plate. The plate was made to be readily removable from the duct proper (actually, in a few seconds) to provide access to the interior of the duct. This access enabled the assembly and disassembly of the smooth wall as well as the installation and removal of the modules and the barrier(s).

Two types of mass transfer boundary conditions were employed at the module-covered wall. To model the situation where heat transfer occurs, the modules were of naphthalene, cast as described in [3]. The wall on which the modules rested was of aluminum and did not participate in the mass transfer. However, had it been made of naphthalene and participated, its mass transfer would have been small compared with that of the modules. The other boundary condition at the module-covered wall was zero mass transfer (i.e. zero heat transfer). This condition was achieved by the use of modules made of brass. The barriers were made of plexiglass and did not participate in the mass transfer.

To complete the description of the test section, it remains to specify the dimensions. For generality, these may be stated as dimension ratios:

$$t/L = 0.375, \quad t/(H+t) = 0.358,$$

$$S/L = 0.250, \quad P/H = 1.83,$$

$$W/H = 7.33, \quad B/H = 0.183 \text{ and } 0.366$$

where $P = L+S$. Certain of the dimensions will also appear in the Reynolds and Sherwood numbers.

The test section was fed by a smooth-walled rectangular duct, hereafter termed the upstream delivery duct. The cross-section of the delivery duct was essentially equal to that of the test section in the absence of the modules. Therefore, with the modules present, the airflow experienced an abrupt contraction in cross-section in passing from the delivery duct into the test section. This occurrence is consistent with practice, where some sort of flow disturbance at the beginning of the module array is virtually inevitable. In view of this, mass transfer coefficients were evaluated only at smooth-wall segments situated well downstream of the beginning of the array, where the disturbances due to the abrupt contraction had died away.

The airflow leaving the test section experienced an abrupt enlargement as it discharged into a rectangular duct whose cross-section equalled that of the upstream delivery duct. Correspondingly, data were not collected at the last segment of the smooth wall.

The system was operated in the suction mode, in which air drawn from the temperature-controlled laboratory passed through the upstream delivery duct, the test section, and the downstream discharge duct. The air was then conveyed to a flowmeter (a calibrated orifice), a control valve, and a blower. The blower was situated in a service corridor outside the laboratory, and its naphthalene-enriched discharge was vented outside the building.

Experimental procedure

The primary quantity needed in the evaluation of the mass transfer coefficient at each of the segments of the smooth wall is the per-segment change of mass during a data run. This information was obtained from precise weighings of each segment immediately before and immediately after the run. For those data runs where mass transfer also occurred at the modules, the change of mass of each module was also determined. The mass measurements were accomplished with a Sartorius ultra-precision electronic balance having a resolution of 0.00001 g. The measured changes of mass were typically in the 0.02–0.06-g range.

Another quantity needed in the data reduction is the naphthalene vapor density at the smooth wall of the duct. Under the assumption that solid–vapor equilibrium exists at the subliming surface, the vapor density is a unique function of the surface temperature. As noted earlier, thermocouples were installed in two of the naphthalene slabs which made up the smooth wall. The thermocouples had been precalibrated, and their emfs were read to 1 μV.

To obtain results of consistently high accuracy, the temperature of the subliming surfaces should be steady, since a steady temperature makes for steady values of the equilibrium naphthalene vapor density and of mass transfer rate. To ensure that steady-state conditions prevailed during the data runs, each run was preceded by an equilibration period.

Data reduction

The distribution of the quasi-local mass transfer coefficient along the smooth wall was determined by evaluating the average coefficient at each of the individual segments which comprised the wall. In this regard, consider any typical segment i, at which the average mass transfer coefficient K_i is defined as

$$K_i = (\dot{M}_i/A_i)/\Delta\rho_{n,i}. \tag{1}$$

In this equation, $\dot{M}_i$ is the rate of mass transfer, A_i is the transfer surface area, and $\Delta\rho_{n,i}$ is the difference in the naphthalene vapor densities at the wall and in the bulk, all at segment i.

The mass transfer rate $\dot{M}_i$ was evaluated as the ratio $\Delta M_i/\tau$, *where* ΔM_i is the change of mass during the run and τ is the duration of the run. The density difference $\Delta\rho_{n,i}$ may be written explicitly as

$$\Delta\rho_{n,i} = (\rho_{nw}-\rho_{nb})_i. \tag{2}$$

For the naphthalene vapor density ρ_{nw} at the wall, the vapor pressure–temperature relation [4] was used in conjunction with the perfect gas law, with the measured wall temperature being used as input. Temperature uniformity prevailed along the wall, so that ρ_{nw} had the same value at all the segments for a given data run.

The bulk density of the naphthalene vapor is zero at the inlet of the test section and increases in the streamwise direction as the airflow is enriched with vapor due to sublimation at the segments of the smooth wall and at the modules, if they are mass transfer active. In general, if naphthalene vapor is added at a rate $\dot{M}$ to an airflow whose volume flowrate is $\dot{Q}$, the increase in the vapor density is given by

$$\Delta\rho_{nb} = \dot{M}/\dot{Q}. \tag{3}$$

If a separate accounting is made of the mass added to the airflow at the segments and at the modules, there follows

$$\rho_{nb,i} = (1/\dot{Q})\left[\sum_{j=1}^{i-1}\dot{M}_j+\frac{1}{2}\dot{M}_i\right]_{seg} + (1/\dot{Q})\left[\sum_{j=1}^{i-1}\dot{M}_j+\frac{1}{2}\dot{M}_i\right]_{mod} \tag{4}$$

where, in the second bracket, $\dot{M}_j$ represents the collective rate of mass transfer of the modules in row j.

The first bracket sums the mass transferred at all segments upstream of the ith segment, plus half of the mass transfer at the ith. The second bracket performs the same function for the modules (if they are mass transfer active), where it may be noted that the ith segment and the ith row of modules are abreast. Note also that the volume flowrate $\dot{Q}$ was virtually constant along the test section (typically less than 0.1% variation).

Once the individual-segment mass transfer coefficients have been evaluated, they may be recast in dimensionless form in terms of the Sherwood number. The duct height H was chosen as the characteristic dimension in the Sherwood number. Since H was

constant throughout the experiments, variations in the Sherwood number are true reflections of variations in the mass transfer coefficient. The Sherwood number definition is

$$Sh = KH/\mathscr{D} \tag{5}$$

from which the mass diffusion coefficient $\mathscr{D}$ can be eliminated via the Schmidt number ($Sc = \nu/\mathscr{D}$), so that

$$Sh = (KH/\nu)Sc. \tag{6}$$

For naphthalene diffusion in air, $Sc = 2.5$ [4].

The Sherwood number results will be presented as a function of the Reynolds number, which is defined here as

$$Re = V^*H/\nu. \tag{7}$$

The quantity V^* is a superficial velocity based on the air flowrate $\dot{w}$ and on the cross-sectional area WH between the tops of the modules and the smooth wall (thereby ignoring the intermodule gaps), so that

$$V^* = \dot{w}/\rho(WH). \tag{8}$$

Elimination of V^* yields

$$Re = \dot{w}/\mu W. \tag{9}$$

Thus, since the duct width W was constant throughout the experiments, the Reynolds number can be regarded as a dimensionless mass flowrate.

RESULTS AND DISCUSSION

The presentation of the smooth-wall mass transfer coefficients (Sherwood numbers) will be made in two parts. In the first, results will be reported for the case in which there are no enhancement barriers in the test section. The second part of the presentation will be focused on the effects of barriers on the smooth-wall mass transfer.

Smooth-wall Sherwood numbers

Streamwise distributions of the Sherwood number are plotted as a function of position along the smooth wall of the duct in Figs. 2 and 3. Each data point

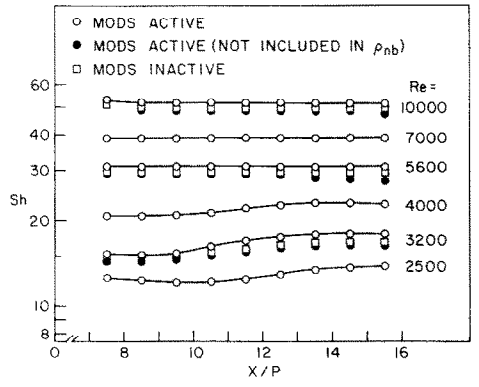

FIG. 2. Smooth-wall Sherwood numbers (mass transfer at both the smooth wall and the modules).

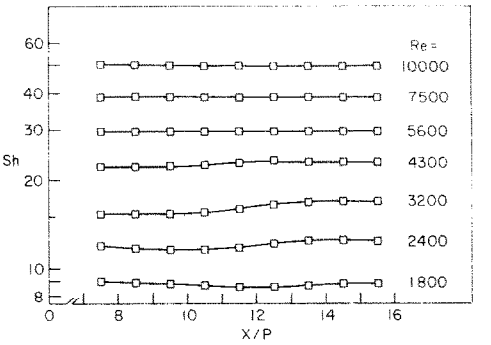

FIG. 3. Smooth-wall Sherwood numbers (mass transfer at the smooth wall but not at the modules).

represents the average Sherwood number for an individual segment and is plotted at the streamwise midpoint of the segment. The streamwise coordinate is X, with $X = 0$ corresponding to the onset of mass transfer at the smooth wall as well as to the beginning of the module array. Note that X is made dimensionless with respect to the period length P of the module array. The first data point corresponds to the segment which is situated between $X = 7P$ and $8P$. Sherwood numbers were not evaluated for smaller X because of the possible intrusive effects of the contraction of the flow cross-section at $X = 0$.

In each figure, the axial distributions are parameterized by the Reynolds number. Figure 2 conveys results for the case (represented by the open-circle data symbols) where mass transfer occurs at the modules as well as at the smooth wall and also contains supplemental data for comparison purposes. In Fig. 3, the data correspond to the case where there is no mass transfer at the modules. In both figures, smooth curves have been faired through the data for continuity.

Attention will first be focused on Fig. 2 and on the main set of data depicted by the open circles. At the higher Reynolds numbers ($Re = 5600$, 7000 and 10,000), the Sherwood number is altogether independent of the streamwise coordinate, indicating the existence of fully developed conditions. At the lower Reynolds numbers, the Sherwood number distributions increase at first and then level off. This behavior is reminiscent of the final stages of laminar-to-turbulent transition in tube and duct flows.

Consider next the supplementary data (all for the smooth-wall Sherwood number) plotted in Fig. 2 for a representative subset of the investigated Reynolds numbers. The square data symbols, taken from Fig. 3, are for the case where there is no mass transfer at the modules. The black circles (in common with the open circles) correspond to mass transfer at both the smooth wall and the modules, but the module mass transfer has not been included in the evaluation of the bulk naphthalene vapor density ρ_{nb} (i.e. the second bracket of equation (4) has been suppressed).

The relationship between the three sets of data for a given Reynolds number will now be discussed. Envision first the situation where mass transfer occurs

only at the smooth wall (square data symbols). Then, with everything else held fixed, suppose that mass transfer is begun and maintained at the modules. The naphthalene vapor sublimed from the now active modules enriches the airflow, resulting in a reduction of the mass transfer at the smooth wall. This is evidenced by the black-circle data symbols, which reflect the drop in mass transfer rate but do not take the enrichment of ρ_{nb} into account. If the contribution of the modules to ρ_{nb} is taken into account, the Sherwood numbers increase from the black-circle to the open-circle data symbols. Note that the open circles lie above the square data symbols, that is, the Sherwood numbers in the presence of mass transfer at both principal walls exceed those for mass transfer at the smooth wall alone. The difference is, however, only about 5%. This trend is consistent with the literature on smooth-walled flat rectangular ducts, where the Nusselt (Sherwood) numbers for symmetrical heating exceed those for unsymmetrical heating [5, 6].

The streamwise distributions of Fig. 3 are very similar to those of Fig. 2 but with slightly lower values of the Sherwood number as discussed in the preceding paragraph. Also, the undulation of the developing Sherwood number distributions at the lower Reynolds numbers is somewhat muted.

It is relevant to compare the results for the present duct whose principal walls have distinctly different geometries with literature results for conventional smooth-walled ducts. To facilitate the comparison, it is necessary to rephrase the present Sherwood and Reynolds numbers to incorporate the hydraulic diameter as the characteristic length. Owing to the presence of the intermodule gaps, there is an uncertainty about how to define the hydraulic diameter. Consistent with the definition of V^* [equation (8)], the hydraulic diameter will be defined for a rectangle of height H and width W (the cross-section between the tops of the modules and the smooth wall). If Sh_D and Re_D denote the Sherwood and Reynolds numbers based on the hydraulic diameter and with $D = 4HW/2(H+W)$, it follows that

$$Sh_D = [2/(1+H/W)]Sh,$$
$$Re_D = [2/(1+H/W)]\,Re \qquad (10)$$

where the bracketed factor is equal to 1.76 for the present apparatus.

The available experimental results for naphthalene sublimation in smooth-walled flat rectangular ducts are for $Re_D \geqslant 10{,}000$ [6], which corresponds to $Re \geqslant \sim 5600$. The fully developed (subscript fd), smooth-wall Sherwood numbers for the three largest Reynolds numbers of the present investigation are brought together in Fig. 4 with the fully developed Sherwood numbers of ref. [6].

The present results plotted in Fig. 4 include both the cases of mass transfer and no mass transfer at the modules, while those of [6] include both one-sided and two-sided heating. Also plotted in Fig. 4 is the Petukhov–Popov semi-empirical correlation for fully developed turbulent heat transfer in a uniformly heated circular tube. In employing the correlation, the Nusselt and Prandtl numbers were replaced by the Sherwood and Schmidt numbers, and the Schmidt number was set equal to 2.5.

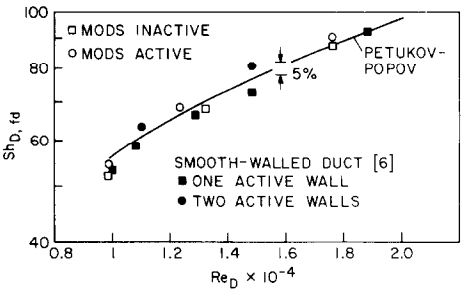

FIG. 4. Comparison of fully developed Sherwood numbers with literature information.

As seen in Fig. 4, the level of agreement between the present Sherwood numbers and those for the smooth-walled flat rectangular duct is remarkably good, especially considering the differences in the physical systems being compared. The major difference is the complex geometry of the module-covered wall. The complex geometry not only affects the velocity field, but it also raises questions about how to define the characteristic velocity and the hydraulic diameter. Judging by the agreement evidenced in Fig. 4, the decision to base both definitions on the cross-section contained between the tops of the modules and the smooth wall was a good one. The effectiveness of the Petukhov–Popov circular tube correlation in predicting the present results is also remarkable.

Barrier-related phenomena

The configuration of the test section with a barrier in place is illustrated in Fig. 1(a). Experiments were performed using either a single barrier, as in the figure, or a pair of barriers separated by either one, two or three modules. Two barrier heights were employed, respectively $B/H = 0.183$ and 0.366. All of the experiments involving barriers were carried out without mass transfer at the modules.

The barrier-affected Sherwood number results display a number of novel features which will be identified and rationalized in this section of the paper. The next section is more focused on the results themselves.

The presentation begins with Fig. 5, which corresponds to the presence of a single $B/H = 0.183$ barrier. As illustrated in the figure adjacent to the abscissa axis. the barrier was located between module rows 9 and 10. The smooth-wall Sherwood number distributions, expressed as the ratio Sh/Sh_{fd}, are plotted for Reynolds numbers of 1800, 3200, 5600 and 10,000.

From the figure, it is seen that the effect of the barrier propagates upstream, causing the Sherwood number to increase in the streamwise direction. Just after the barrier, the Sherwood number drops and attains a

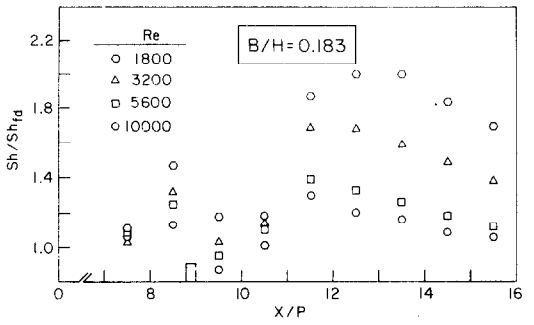

FIG. 5. Sherwood numbers in the presence of a single $B/H = 0.183$ barrier.

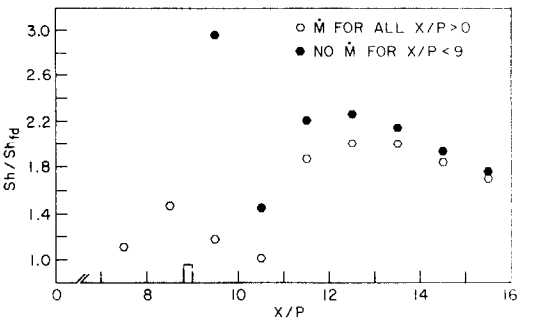

FIG. 6. Comparison of Sherwood numbers with and without mass transfer upstream of a single $B/H = 0.183$ barrier, $Re = 1800$.

minimum. Thereafter, it increases to a downstream maximum, whereafter it decreases again. This complex distribution contains many unexpected features, particularly the post-barrier decrease and minimum, the subsequent increase, and the downstream positioning of the maximum. A more expected distribution would have included the pre-barrier increase (due to the precursive acceleration of the flow), a further increase just downstream of the barrier as the flow continues to contract and accelerate, a maximum at the vena contracta point, and a subsequent decrease which accompanies the expansion and deceleration of the flow after the vena contracta.

The noteworthy features of the measured Sherwood number distributions will now be rationalized. It may be hypothesized that the post-barrier minimum is caused by a zone of high naphthalene vapor concentration situated adjacent to the portion of the wall where the minimum occurs. Such a high concentration may be created when naphthalene vapor sublimed at segments upstream of the barrier is forced against the wall by the upwelling of the flow at the barrier.

To examine this hypothesis, the experiments of Fig. 5 were repeated but with mass transfer suppressed at all segments upstream of the barrier, so that the flow arriving at the barrier was free of naphthalene vapor. Data from these experiments are plotted as black symbols in Figs. 6 and 7, respectively for $Re = 1800$ and 5600 (the results for the other Reynolds numbers are available in [3]). For comparison purposes, the data from Fig. 5 have also been plotted in Figs. 6 and 7 (open symbols).

In either of Figs. 6 and 7, if attention is focused on the first segment after the barrier (i.e. on the data at $X/P = 9.5$), it is seen that the black data point falls very much higher than the open data point, and, in fact, marks the maximum in the Sh/Sh_{fd} distribution. Note also that at a given Reynolds number, the two sets of data correspond to identical hydrodynamics and differ only due to the upstream mass transfer condition. Therefore, it may be concluded that the drop in the Sherwood number immediately after the barrier, evidenced in Fig. 5 and by the open symbols of Figs. 6 and 7, was due to vapor blanketing, as hypothesized.

Further examination of Figs. 6 and 7 indicates that phenomena additional to vapor blanketing are needed to fully explain the trends in the Sh/Sh_{fd} distributions of Fig. 5. Of particular note in Figs. 6 and 7 is the dropoff of the black data points between the first and second segments after the barrier, the minimum attained at the second segment (i.e. at $X/P = 9.5$), and the subsequent increase. The dropoff cannot be due to vapor blanketing, since upstream mass transfer was suppressed. Rather, the dropoff, the minimum, the subsequent increase, and the maximum are believed due to flow separation and reattachment processes.

Specifically, flow visualizations performed in ref. [2] demonstrated that the flow, which was forced to separate from the module-covered wall due to the presence of the barrier, reattached to that wall between $X/P = 10$ and 11. It is believed that the reattachment at the module-covered wall is accompanied by separation at the smooth wall. The separation is caused by the adverse pressure gradient associated with the deceleration of the flow, and its presence is the cause of the low value of the Sherwood number at $X/P = 10.5$. This hypothesis is supported by the findings of ref. [6], where mass transfer was investigated in a parallel-walled channel bounded by a smooth wall and an opposite wall covered with low-profile periodically positioned barriers. It was found that the smooth-wall mass transfer was a minimum at streamwise stations at which the flow reattached on the barrier-covered wall.

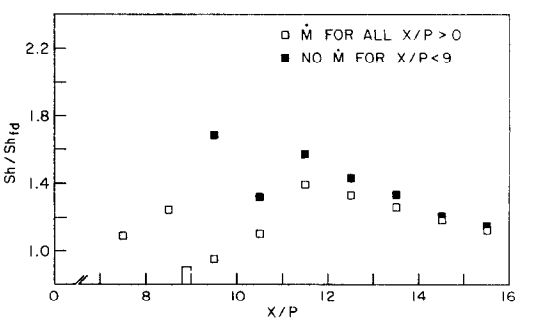

FIG. 7. Comparison of Sherwood numbers with and without mass transfer upstream of a single $B/H = 0.183$ barrier, $Re = 5600$.

The presence of the separation bubble adjacent to the smooth wall also explains the post-minimum rebound and the subsequent maximum in the Sherwood number distributions. The rebound is due to the narrowing of the bubble as the reattachment point is approached, and the maximum occurs at reattachment (not at the vena contracta). The dropoff of the Sherwood number downstream of the reattachment is caused by the redevelopment of the fluid flow and mass transfer boundary layers.

All of the noteworthy features of the Sherwood number distributions of Fig. 5 have now been rationalized. Further inspection of that figure suggests that the post-barrier minimum and maximum in each distribution tend to shift upstream as the Reynolds number increases. This trend is believed due to the sharper turns executed both upstream and downstream of the barrier by the higher Reynolds number flows.

As a final item in the examination of barrier-related phenomena, a series of experiments was performed to clarify the post-barrier maximum which occurs in the absence of mass transfer upstream of the barrier (i.e. in Figs. 6 and 7, the black data points at $X/P = 9.5$). The matter at issue is whether the maximum is primarily due to the thin mass transfer boundary layer or to the heightened velocity of the flow caused by the presence of the barrier.

To investigate this issue, data were collected without a barrier and for no mass transfer upstream of the site vacated by the barrier. Representative Sherwood number distributions for this case are plotted as open symbols in Fig. 8. For comparison, the black symbols from Figs. 6 and 7 (barrier in place, no mass transfer upstream of barrier) are also plotted in Fig. 8.

The no-barrier results display the traditional entrance-region monotonic decrease with increasing downstream distance, a trend which contrasts sharply with the undulating distribution which exists in the presence of the barrier. More to the point, it is seen that the black data symbols at the first post-barrier segment (i.e. at $X/P = 9.5$) fall higher than those for the no-barrier case. The vertical gap between the symbols reflects the enhancement provided by the heightened velocity due to the barrier. This effect is seen to be more

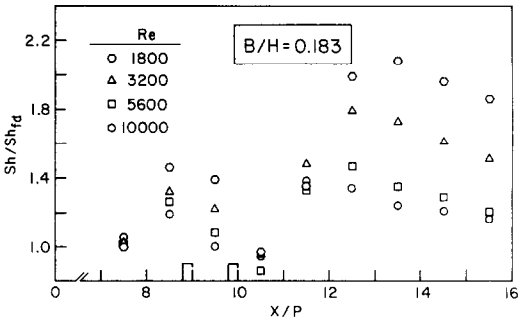

FIG. 9. Sherwood numbers in the presence of a pair of $B/H = 0.183$ barriers separated by one row of modules.

marked at the lower Reynolds numbers and dies away as the Reynolds number increases.

Barrier-affected Sherwood numbers

The smooth-wall Sherwood number results for all of the investigated barrier configurations will now be presented. Returning to Fig. 5 (single barrier, $B/H = 0.183$), it is relevant to take note of the extent of the barrier-related enhancement (relative to Sh_{fd}). The greatest enhancement occurs at the lowest Reynolds number and is about a factor of two. The enhancement decreases markedly as the Reynolds number increases so that, for example, the largest enhancement at $Re = 10{,}000$ is 1.3. Because of the complex phenomena discussed in the preceding section of the paper, the major zone of enhancement is displaced downstream from the immediate neighborhood of the barrier. There is also a weaker, narrow zone of enhancement just upstream of the barrier.

Attention is now turned to the Sherwood number results in the presence of two $B/H = 0.183$ barriers, and Figs. 9–11 have been prepared for this purpose. The successive figures correspond to barriers which are separated by one, two, and three modules.

A comparison of the results in Fig. 9 (most closely spaced barrier pair) with those in Fig. 5 (single barrier) reveals a clear similarity in the undulating shapes of the streamwise distributions. Not unexpectedly, the main

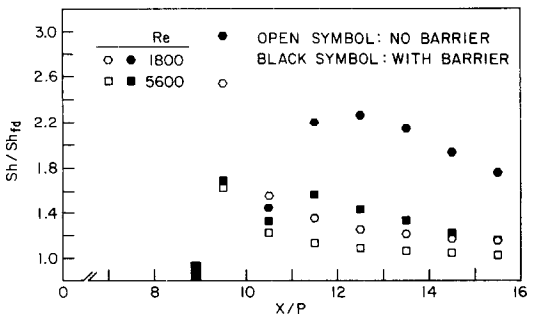

FIG. 8. Comparison of Sherwood number distributions with and without a barrier (no mass transfer for $X/P < 9$).

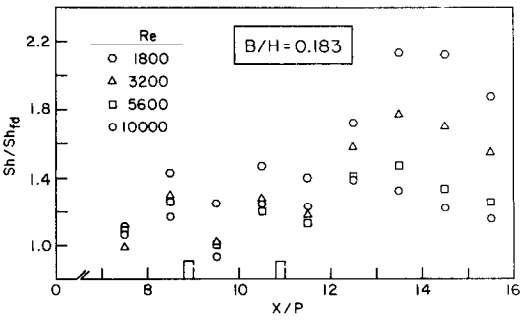

FIG. 10. Sherwood numbers in the presence of a pair of $B/H = 0.183$ barriers separated by two rows of modules.

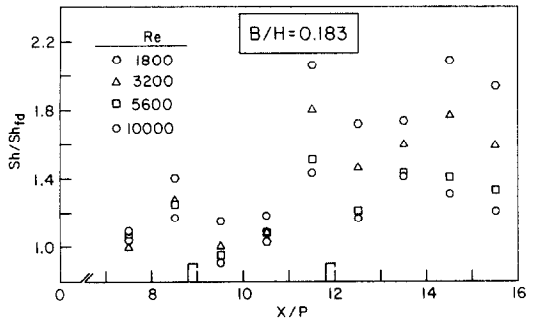

FIG. 11. Sherwood numbers in the presence of a pair of $B/H = 0.183$ barriers separated by three rows of modules.

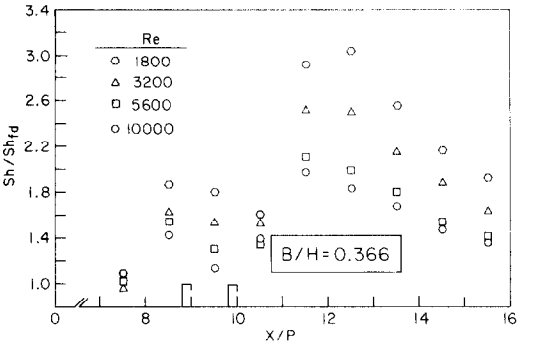

FIG. 13. Sherwood numbers in the presence of a pair of $B/H = 0.366$ barriers separated by one row of modules.

differences between the two sets of results are encountered at $X/P = 9.5$, 10.5, and 11.5, where the vapor blanketing and flow separation occur. In the downstream region, the enhancement of the Sherwood number in the presence of the barrier pair is moderately larger than that in the presence of the single barrier.

The Sh/Sh_{fd} distributions become more complex as the separation between the barriers increases, as can be seen in Figs. 10 and 11. In each figure, there are three local maxima in each distribution, rather than two as before. The new maximum, which occurs in the downstream portion of the interbarrier zone, is a fledgling in Fig. 10 but attains a towering stature in Fig. 11, indicative of flow reattachment.

To complement the three local maxima, there are now two local minima in each distribution, one downstream of each barrier. It may be noted that the second minimum is not as low as the first minimum, probably because the double-barrier-induced turbulence moderates the vapor blanketing. This higher turbulence level is also believed to be the cause of the moderate increases in the downstream-region enhancements relative to those for the single barrier.

The barrier-affected Sherwood numbers presented up to now have been for the lower of the two investigated barrier heights, namely, $B/H = 0.183$. Attention will now be turned to the higher barrier, which is characterized by $B/H = 0.366$.

The Sherwood number distributions in the presence of a single $B/H = 0.366$ barrier are displayed in Fig. 12.

These distributions are characterized by undulations similar to those already discussed in connection with the single $B/H = 0.183$ barrier of Fig. 5. A comparison of Figs. 5 and 12 shows that the higher barrier gives rise to substantially greater enhancements than the lower barrier. For example, for $Re = 1800$, the enhancement peak for the higher barrier is $Sh/Sh_{fd} \cong 3.4$, while that for the lower barrier is $Sh/Sh_{fd} = 2.0$. The corresponding comparison for $Re = 10{,}000$ yields 2.0 and 1.3. Even upstream, the enhancements induced by the higher barrier are substantial, ranging from 1.4 to 1.9. Note also that the post-barrier minimum is not as deep for the higher barrier as for the lower barrier.

The Sherwood number distributions corresponding to the most closely spaced pair of $B/H = 0.366$ barriers are presented in Fig. 13. These distributions are very similar to those of Fig. 12 for the single barrier. The presence of the second barrier tends to postpone the post-barrier rebound and, for the lower Reynolds numbers, to slightly increase the Sherwood number enhancement in the downstream region.

With the widening of the interbarrier separation (Figs. 14 and 15), significant enhancement occurs at streamwise stations in the downstream portion of the interbarrier zone. Furthermore, the post-barrier dropoff downstream of the second barrier has virtually disappeared. As a consequence of these features, the downstream zone of high enhancement is broadened and encompasses four or five period lengths.

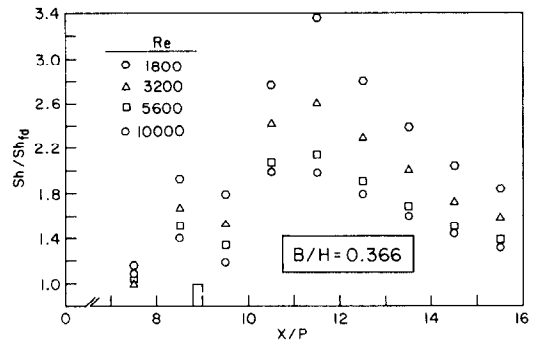

FIG. 12. Sherwood numbers in the presence of a single $B/H = 0.366$ barrier.

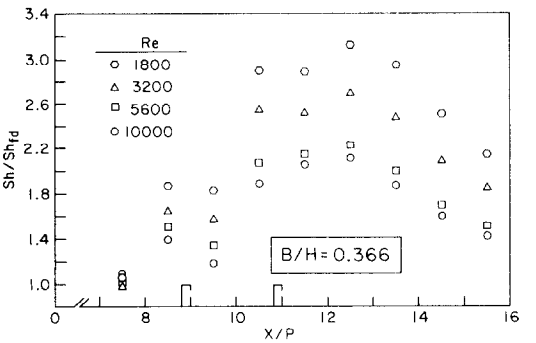

FIG. 14. Sherwood numbers in the presence of a pair of $B/H = 0.366$ barriers separated by two rows of modules.

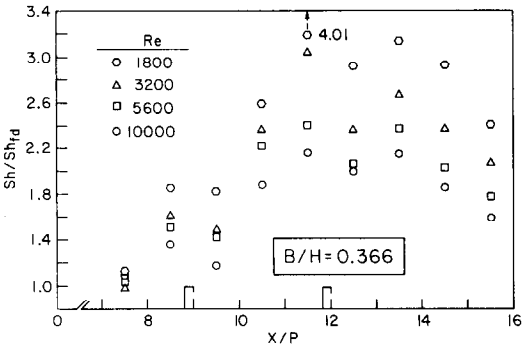

FIG. 15. Sherwood numbers in the presence of a pair of $B/H = 0.366$ barriers separated by three rows of modules.

CONCLUDING REMARKS

The experimental work performed here has provided quasi-local mass (heat) transfer coefficients at the smooth principal wall of a flat rectangular duct whose other principal wall is covered with an array of periodically positioned, blocklike elements (modules). Measurements were made for hydraulic-diameter Reynolds numbers ranging from about 3000 to 18,000. The fully developed Sherwood (Nusselt) numbers were compared with literature information for smooth-walled rectangular ducts, available for Reynolds numbers of 10,000 and greater. When the Sherwood and Reynolds numbers incorporated a hydraulic diameter based on the rectangular cross-section between the tops of the modules and the smooth wall, very good agreement prevailed between the present data and those for smooth-walled ducts.

Experiments were performed in which mass transfer occurred both at the smooth wall and at the module-covered wall, and these were supplemented by experiments where mass transfer occurred only at the smooth wall. The smooth-wall Sherwood numbers in the presence of mass transfer at both walls exceeded, by about 5%, those for mass transfer at the smooth wall alone.

In another facet of the research, the use of barriers to enhance the smooth-wall mass transfer was investigated. The barriers were seated in the space between two successive rows of modules and protruded into the flow passage, directing the airstream toward the smooth wall. Both single barriers and pairs of barriers were employed, with parametric variations of the streamwise separation of the barrier pairs and for two different barrier heights.

Substantial enhancement was achieved by the use of barriers, especially at the lower Reynolds numbers and for the higher barriers. Contrary to expectations, the major enhancement did not occur immediately downstream of a barrier. Rather, a local mass transfer minimum existed in that region owing to the presence of a high concentration of naphthalene vapor and to flow separation. The peak enhancement occurred further downstream, at the point where the separated flow reattached to the smooth wall.

REFERENCES

1. E. M. Sparrow, A. A. Yanezmoreno and D. R. Otis, Jr., Convective heat transfer response to height differences in an array of block-like electronic components, *Int. J. Heat Mass Transfer* **27**, 469–473 (1984).
2. E. M. Sparrow, S. B. Vemuri and D. S. Kadle, Enhanced and local heat transfer, pressure drop, and flow visualization for arrays of block-like electronic components, *Int. J. Heat Mass Transfer* **26**, 689–699 (1983).
3. D. R. Otis, Jr., Heat transfer at the smooth and the block-covered walls of a flat rectangular duct, M. S. thesis, Department of Mechanical Engineering, University of Minnesota, Minneapolis, Minnesota (1984).
4. H. H. Sogin, Sublimation from disks to air streams flowing normal to their surfaces, *Trans. Am. Soc. mech. Engrs* **80**, 61–71 (1958).
5. E. M. Sparrow, J. R. Lloyd and C. W. Hixon, Experiments on turbulent heat transfer in an asymmetrically heated rectangular duct, *J. Heat Transfer* **88**, 170–174 (1966).
6. E. M. Sparrow and W. Q. Tao, Enhanced heat transfer in a flat rectangular duct with streamwise-periodic disturbances at one principal wall, *J. Heat Transfer* **105**, 851–861 (1983).

TRANSFERT THERMIQUE POUR UN ECOULEMENT DANS UN CANAL DONT UNE PAROI LISSE FAIT FACE A UNE PAROI COUVERTE DE PROTUBERANCES

Résumé—Des mesures sont faites pour déterminer des coefficients de transfert thermique presque local sur la paroi lisse d'un canal plat rectangulaire dont l'autre paroi est recouverte par un arrangement d'éléments en bloc (dénommés modules). Le nombre de Reynolds de diamètre hydraulique varie entre 3000 et 18000. Les nombres de Nusselt pleinement établis sont bien en accord avec ceux des canaux à parois lisses, lorsque le diamètre hydraulique est calculé à partir de la distance entre les sommets des modules et la paroi lisse. Le chauffage simultané à la paroi lisse et aux modules conduit à des coefficients légèrement supérieurs que pour la surface lisse chauffée seule. On étudie l'accroissement du transfert sur la paroi lisse avec des barrières placées dans l'espace entre les allées successives des modules. Un accroissement substantiel est obtenu aux nombres de Reynolds les plus faibles et pour les barrières les plus hautes. L'accroissement le plus élevé n'est pas réalisé immédiatement derrière une barrière mais plutôt plus loin en aval au point où l'écoulement séparé induit par la barrière s'attache à nouveau à la paroi lisse.

WÄRMEÜBERTRAGUNG AN DER GLATTEN WAND EINES KANALS, DIE SICH GEBENÜBER EINER MIT HÖCKERN BEDECKTEN WAND BEFINDET

Zusammenfassung—Es wurden Messungen durchgeführt, um den quasi-lokalen Wärmeübergangskoeffizienten an einer glatten Grundseite eines flachen rechteckigen Kanals zu bestimmen, dessen andere Grundseite durch eine Anordnung von blockähnlichen Elementen (bezeichnet als Module) bedeckt ist. Die mit dem hydraulischen Durchmesser berechnete Reynolds-Zahl liegt im Bereich von ca. 3000 bis 18000. Die für vollständig ausgebildete Strömung bestimmten Nusselt-Zahlen stimmen mit denen für glattwandige Kanäle gut überein, wenn der hydraulische Durchmesser für den rechteckigen Querschnitt zwischen den Spitzen der Module und der glatten Wand berechnet wird. Die Beheizung der glatten Wand sowie der Module ergibt einen wenig höheren Wärmeübergangskoeffizienten als bei Beheizung der glatten Wand allein. Die Erhöhung der Wärmeübertragung an der glatten Wand durch Anbringen von Hindernissen im Raum zwischen den aufeinanderfolgenden Reihen von Modulen wurde untersucht. Beträchtliche Erhöhungen wurden bei niedrigen Reynolds-Zahlen und für hohe Hindernisse erzielt. Die größte Steigerung erfolgte nicht sofort nach einem Hindernis, sondern weiter stromabwärts an dem Punkt, an dem die durch das Hindernis abgelöste Strömung sich wieder an die glatte Wand anlegt.

ТЕПЛООБМЕН В КАНАЛЕ У ГЛАДКОЙ СТЕНКИ, ОБРАЩЕННОЙ К СТЕНЕ С ШЕРОХОВАТОСТЯМИ

Аннотация—Измерены коэффициенты квази-локального теплообмена у гладкой основной стенки плоского прямоугольного канала, другая основная стенка которого покрыта решеткой из блоков (так называемых модулей). Число Рейнольдса, определенное по гидравлическому диаметру, изменялось от 3000 до 18000. Числа Нуссельта полностью развитого потока хорошо согласовывались с их значениями для гладкостенных каналов, когда гидравлический диаметр определялся по прямоугольному сечению между вершинами модулей и гладкой стенки. Нагрев как гладкой стенки, так и модулей приводил лишь к несколько большим значениям коэффициентов (в отличие от нагрева только гладкой стенки). Исследовалось усиление теплообмена гладкой стенки, вызванное установкой перегородок в пространстве между последовательными рядами модулей. Существенное увеличение было достигнуто при меньших числах Рейнольдса и при более высоких перегородках. Наибольшее усиление возникает не сразу за перегородкой, но скорее дальше вниз по потоку в точке, где оторвавшийся от перегородки поток присоединяется к гладкой стенке.